31st International Conference Nuclear Energy for New Europe
NENE 2022 September 12-15 PORTOROŽ SLOVENIA

Towards More Ductile Refractory High-Entropy Alloys At Room Temperature

Sal Rodriguez[1]
[1]Sandia National Laboratories
PO Box 5800
Albuquerque, NM, USA 87185
sbrodri@sandia.gov

Rob Sharpe[1], Erin Barrick[1], Darryn Fleming[1], Andrew Kustas[1], Nima Fathi[2], Eric Lang[3], Levi Van Bastian[1], and Graham Monroe[1]

[2]Texas A&M University, 200 Seawolf Parkway, Galveston, Texas, 77554
[3]1 University of New Mexico, MSC01 1100, Albuquerque, New Mexico, USA, 87131

rasharp@sandia.gov[1], ejbarri@sandia.gov[1], ddflemi@sandia.gov[1], akustas@sandia.gov[1], nfathi@tamu.edu[2], ejlang2@unm.edu[3], ldvanba@sandia.gov[1], gmonroe@sandia.gov[1]

ABSTRACT

Refractory high-entropy alloys (RHEAs) typically consist of four or more refractory elements, usually in equiatomic proportions. Consequently, many RHEAs tend to have high yield strength at elevated temperature. An additional benefit of high-entropy is the solid solution mixing that can provide alloy cohesion and integrity that generates corrosion-resistant layers and self-healing. However, as noted over the past few years, the number of RHEAs with ductile properties at room temperature (RT) is rather scarce, with fewer than 1% of RHEAs achieving this metric; most RHEAs are notoriously brittle at room temperature, though fortunately, there are exceptions. Ductility is a key goal for widespread commercial RHEA manufacturing because it is intricately associated with machinability of industrial components. Certainly, high-strength ductile (HSD) RHEAs are of much interest to the nuclear industry and other energy sectors, as well as aerospace and transportation.

Here, a search of the literature associated with HSD RHEAs at RT was conducted, fully realizing that the field continues to grow at an accelerated pace, so it is nearly impossible to find all such references. In any case, a key RHEA researcher noted in 2018 that just HfNbTaTiZr and a few of its derived, hybrid combinations fulfilled such metric. Herein, four years later, 17 such combinations were identified in the literature. A table with the potentially-HSD RHEAs was compiled, and the following RHEAs were manufactured using the advanced manufacturing methods of spark plasma sintering (SPS) and laser engineered net shaping (LENS): $AlNbTiVZr_{1/2}$, CrMoNbTaV, CrMoVW, HfMoNbTiZr, HfNbTiV, HfNbTiVZr, $Hf_{1/2}Nb_{1/2}Ta_{1/2}Ti_{3/2}Zr$, MoNbTiVZr, $Mo_{1/2}NbTiW_{1/2}$, NbTaTiV, and $NbTiV_2Zr$. Then, the RHEAs underwent a series of tests to assess their relative strength, ductility, and machinability. The machining performed to date includes drilling, lathing, slicing, welding, and filing. Of the 11 RHEAs, the following seven had the highest degree of machinability: CrMoNbTaV, CrMoVW, HfNbTiV, MoNbTiVZr, $Mo_{1/2}NbTiW_{1/2}$, NbTaTiV, and $NbTiV_2Zr$. Finally, a synthesis of the experimental data, elemental combinations, material properties, and

machinability provided insights regarding HSD RHEA compositions and pathways for improving ductility at RT.

1 INTRODUCTION

The advent of refractory high-entropy alloys (RHEAs) in 2010 for high-temperature aerospace applications resulted in a flurry that generated thousands of research papers and thousands of RHEA combinations [1-5]. RHEAs typically consist of four or more refractory elements (e.g., HfNbTaTiZr), usually in equiatomic proportions. However, some variants include aluminum, nickel, and silicon (e.g., AlNbTiVZr), while others have non-equiatomic proportions (e.g., $MoNb_{1/3}Ti_{1/3}V_{1/3}Zr$). Some RHEA combinations have shown remarkable properties that exceed the performance of Inconel 718, such as high-strength at elevated temperature, corrosion resistance, erosion resistance, and self-healing. However, it is noted in metallurgy that materials with high strength tend to have reduced ductility, and the converse is also true. Hence, not surprisingly, less than 1% of RHEAs have ductile properties at room temperature (RT) [6]. This is the case because most, if not all, primary RHEA structures are body centered cubic (BCC), whereas many face centered cubic (FCC) elements and alloys tend to be ductile and have a low ductile/brittle transition temperature (DBTT) [7]. Note that for this research, the manufactured RHEA specimens were several centimeters long in length and width, as opposed to sub-millimeter RHEA test pieces. Hence, RHEA nanoparticle domains that exhibit high ductility and/or strength, may not necessarily extend their performance onto the macro scale; and that may explain why not all the RHEAs cited in the literature as being ductile passed the machinability tests.

To investigate this situation, a search of the literature was conducted for high-strength ductile (HSD) RHEAs at RT. The authors recognize that the number of RHEA reports is in the thousands, so unfortunately, important HSD RHEA combinations are likely to have been missed. On the bright side, the manufactured sample size provides a reasonable glimpse of ductile RHEAs. Moreover, it is noted that as far as the authors are aware, this document summarizes the longest list of HSD RHEAs found in the literature. For example, a key RHEA researcher noted four years ago that just HfNbTaTiZr and a few of its derived, hybrid combinations were ductile at RT [1].

2 HSD RHEAS IN THE LITERATURE

The 11 RHEAs of interest that were manufactured for this research include:

- $AlNbTiVZr_{1/2}$
- CrMoNbTaV
- CrMoVW
- HfMoNbTiZr
- HfNbTiV
- HfNbTiVZr
- $Hf_{1/2}Nb_{1/2}Ta_{1/2}Ti_{3/2}Zr$
- MoNbTiVZr
- $Mo_{1/2}NbTiW_{1/2}$

- NbTaTiV
- $NbTiV_2Zr$

Other potential HSD RHEAs of interest that will be manufactured soon by our team include:

- NbTiVZr [8]
- HfNbTaTiZr [9, 10]
- HfNbTiZr [11, 12]
- MoNbTiV [13]
- $Mo_{1/3}NbTiV_{1/3}Zr$ [14]
- HfNbTaTiV [15]

3 MANUFACTURED RHEAS AND THEIR PERFORMANCE

The 11 RHEAs were characterized and tested experimentally to determine various key properties associated with ductility (e.g., machinability and Poisson's ratio) and relative strength as measured by the yield strength of the alloy. Ductility is defined as the amount of sustained plastic deformation until failure occurs while the material in question is under tensile stress. Note that the relative capability of RHEAs to withstand drilling represents a significant step towards demonstrating machinability, which is generally a property of ductile materials, because the machined surface tends to have a smooth finish over a range of machining tasks. Drilling was conducted with a 3.18 mm ($1/8^{th}$ inch) drill at 550 RPM. The drill was coated with cobalt carbide, with a hardness of 75 HRC on the Rockwell scale. Because of the hardness of the RHEAs, it was determined that the drill bits should be replaced right after each drill test.

Figure 1 shows typical images under a scanning electron microscope with a 50 microns scale bar for an HfNbTaZr RHEA (left hand side) and the electron backscatter image with the grain structure, with scale bars at 2 and 5 microns. It is noteworthy that the images show a high degree of mixing of the principal elements, which is important to reach the RHEA's optimum strength and ductile properties. The machining performed to date includes drilling, lathing, slicing, welding, and filing. Figure 2 shows some of the recent machining work. Figure 3 shows two fully-completed drill holes on the upper side of an NbTaTiV RHEA. The two holes were drilled completely through the thickness of the RHEA (normal direction), while the partial hole on the left hand side was stopped to show the smooth surface that is generated as the drilling proceeds. Finally, Figure 4 shows various RHEA curls from the drilling operation.

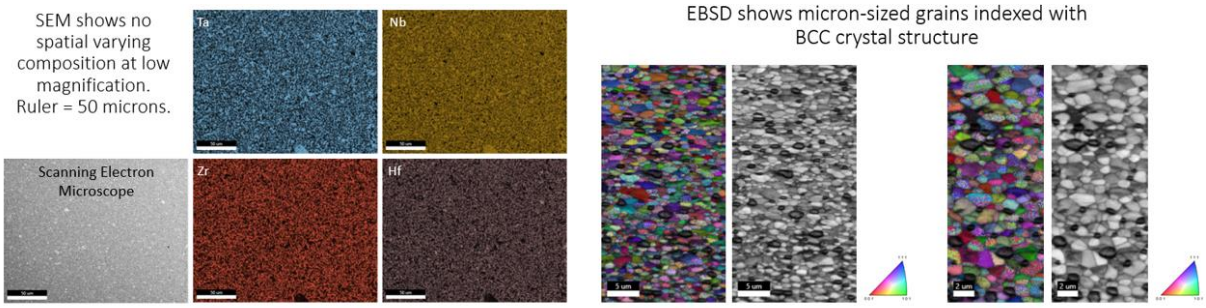

Scanning electron microscope (SEM) image for HfNbTaZr with a ruler scale set to 50 microns.

Electron backscatter diffraction (EBSD) image for HfNbTaZr with a ruler scale set to 2 microns (right) and 5 microns (left).

Figure 1: Scanning electron microscope (left) and two electron backscatter diffraction images for HfNbTaZr RHEAs.

Figure 2: A. Rotating lathe of RHEA tube. B. Drilled and lathed RHEA. C. RHEA to RHEA welding.

Figure 3: Drilled NbTaTiV.

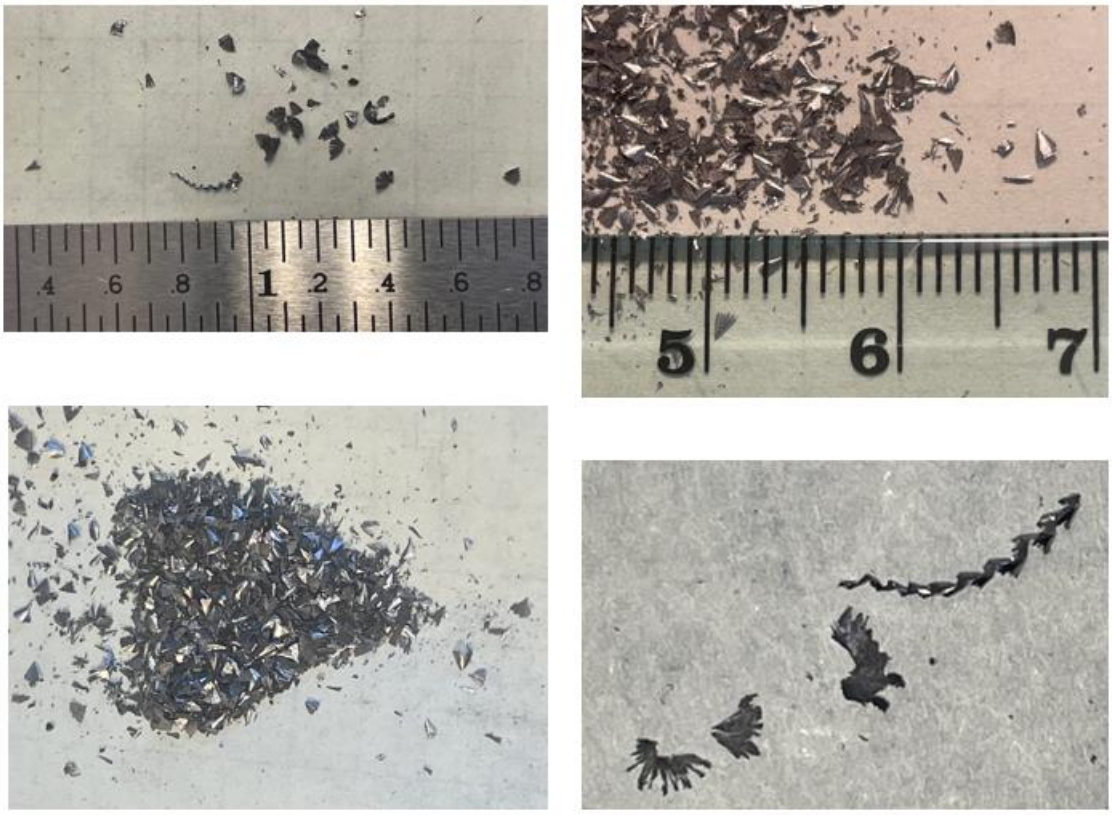

Figure 4: RHEA curls from the drilling operation (the ruler at the left is in inches, while the one on the right is in cm).

Table 1 summarizes the RHEAs that were manufactured for this research, and some of their performance metrics. The RHEAs were recently manufactured using advanced manufacturing by our team via spark plasma sintering (SPS) and laser engineered net shaping (LENS). The SPS samples were 25.4 x 25.4 x 2 mm, while the LENS samples were approximately 10 x 10 x 2 mm. No post-processing was performed on the manufactured samples.

Certainly, many approaches have been employed to both quantify and increase the degree of ductility for a material, e.g., valence electron concentration (VEC) less than 4.4, mixture enthalpy not 'significantly' negative, atomic size differences, elemental intrinsic ductility, Poisson's ratio greater than 0.31, etc. [15, 16, 17]. By contrast, this methodology applies a more pragmatic approach, with the idea that metrics mean little if the alloy is not machinable. For example, a RHEA with a Poisson's ratio greater than 0.31 might theoretically qualify as "ductile" [17]. However, the sample might still shatter into numerous pieces as it is machined for commercialization purposes. Therefore, for conservativeness, the present authors recommend a Poisson's ratio greater than 0.35. Others have considered Mendeleev number sequencing, maximized atomic radii range, Venn diagrams with multiple design criteria, various means to increase entropy while reducing the formation enthalpy, maximum lattice distortion, adding ductilizing elements, and so forth [18-24]. Note that for this research, all RHEAs that showed drillability also displayed machining potential via lathing (e.g., high-speed rotational cutting), slicing via a water jet, and RHEA to RHEA welding [5]. Moreover, the rule of mixtures was used to generate results for Poisson's ratio.

Table 1: Manufactured RHEAs and their performance.

RHEA / References	Manufacturing Method	Poisson's Ratio	Yield Strength at RT (MPa)	Machinable? / Visual results
$AlNbTiVZr_{1/2}$ [14, 22]	SPS	0.36	1,430	Minimal. Generated curls in the range of 0.5 to 2 mm; the opposite surface popped.
CrMoNbTaV [26]	LENS	0.33	1,909	Machinable. Generated smooth drill hole with curls in the range of 0.1 to 1 mm.
CrMoVW [27]	LENS	0.29	1,972	Machinable. Generated smooth drill hole with curls in the range of 0.2 to 1 mm.
HfMoNbTiZr [1, 28]	SPS	0.35	1,719	Minimal. Generated dust and curls in the range 0.1 to 0.2 mm; the opposite surface popped.
$Hf_{1/2}Nb_{1/2}Ta_{1/2}Ti_{3/2}Zr$ [16]	SPS	0.35	903	No. Generated dust; the opposite surface popped. The sample fractured into several pieces.
HfNbTiV [15]	SPS	0.37	1,100	Machinable. Generated smooth drill hole with curls in the range of 0.5 to 2 mm. Top two in terms of machinability.
HfNbTiVZr [1]	SPS	0.37	1,737	No. Generated dust and a few curls up to 0.2 mm; the opposite surface popped. The sample fractured into several pieces.
MoNbTiVZr [14]	SPS	0.33	1,779	Machinable. Generated smooth drill hole with curls in the range of 0.1 to 0.2 mm.
$Mo_{1/2}NbTiW_{1/2}$	SPS	0.33	1,440	Machinable.

[2]				Generated smooth drill hole with curls in the range of 0.5 to 0.2 mm.
NbTaTiV [29]	LENS	0.36	1,273	Machinable. Generated smooth drill hole with curls in the range of 0.25 to 2 mm. Top two in terms of machinability.
$NbTiV_2Zr$ [1]	SPS	0.36	918	Machinable. Generated smooth drill hole with curls in the range of 0.5 to 2 mm.

Of the 11 RHEAs that were manufactured, seven were found to be highly machinable (i.e., CrMoNbTaV, CrMoVW, HfNbTiV, MoNbTiVZr, $Mo_{1/2}NbTiW_{1/2}$, NbTaTiV, and $NbTiV_2Zr$), of which HfNbTiV and NbTaTiV exhibited the highest degree of machinability. In addition, two of the manufactured RHEAs had minimal machinability ($AlNbTiVZr_{1/2}$ and HfMoNbTiZr), and two had no machinability ($Hf_{1/2}Nb_{1/2}Ta_{1/2}Ti_{3/2}Zr$ and HfNbTiVZr).

It is noted that the seven machinable RHEAs generally had Mo, Nb, V, and Ti, with the top two RHEAs involving primarily Nb, Ti, and V. That is not surprising, as Nb, Ti, and V are intrinsically ductile, so adding them to the RHEA cocktail helps induce ductility. By contrast, the top seven RHEAs rarely had Cr, Hf, Ta, W, or Zr; this is confirmed via contrast with the minimal and non-machinable RHEAs, which tended to use Hf and Zr. However, it is noted that relatively pure Hf and Zr are considered ductile. More generally, Group IV (e.g., Ti, Zr, and Hf) and Group V (e.g., V, Nb, and Ta) are intrinsically ductile, while Group VI (e.g., Cr, Mo, and W) is brittle. Thus, additional mechanisms are likely exerting a stronger influence on ductility.

Refractory element combinations with a wide range in radii promote interatomic mixing. It is well-known that Period 6 elements have a larger radius than those in Period 5, which in turn are larger than those in Period 4. Moreover, as the elements move from left to right, the radius becomes smaller. Hence the smallest refractory atoms are those on the right hand side of Period 4 (e.g., Ti, V, Cr, and Mn; Ti is included because its radius is almost the same as that of V), while the largest refractory atoms are those on the left hand side of Period 6 (e.g., Hf, Ta, and W). By applying a Venn diagram for ductility vs. radius range, Ti, V, Hf, and Ta achieve this desirable metric. Thus, RHEA hybrids that use HfTaTiV combinations have a reasonable chance of being ductile, with Nb and Zr being good replacements for Hf and Ta, respectively, given their comparable radius and intrinsic ductility. It is clear that the 17 selected RHEAs have much in common with the selection of HfTaTiV and NbZr, i.e., they are hybrid RHEAs stemming from the senary HfNbTaTiVZr RHEA, which is comparable to the CrMnFeCoNi Cantor high-entropy alloy. Finally, an optimization process involving advanced manufacturing, experiment, theory, and computational modeling can be employed to rapidly prototype and validate the vast potential offered by RHEAs, as only a small fraction has been explored [1, 3, 30].

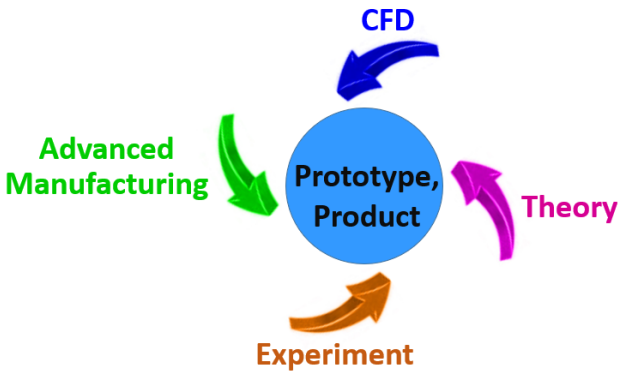

Figure 5: The interplay of advanced manufacturing, experiment, theory, and computational modeling [30].

4 SUMMARY AND CONCLUSION

Eleven RHEAs from the literature were manufactured and tested to evaluate their ductility, machinability, and strength. Of that set, seven were found to be highly machinable. These are the CrMoNbTaV, CrMoVW, HfNbTiV, MoNbTiVZr, $Mo_{1/2}NbTiW_{1/2}$, NbTaTiV, and $NbTiV_2Zr$ RHEAs, of which the most machinable were HfNbTiV and NbTaTiV. Those RHEAs predominantly had Nb, Ti, and V, which are very ductile intrinsically. The atomic size is also found to be relevant towards the degree of ductility, with a wider range of atomic radii being the most favorable. This includes Ti, V, Cr, and Mn from Period 4, and Hf, Ta, and W from Period 6. The refractory elements that have both intrinsic ductility and the widest radii range are Ti, V, Hf, and Ta.

Based on an evaluation of the experimental data, RHEA hybrid combinations that employ some or all of the following elements, Hf, Ta, Ti, and V, have a high likelihood of being ductile; moreover, Nb and Zr can replace Hf and Ta, respectively, given their comparable radius and intrinsic ductility. The data also indicates that the Poisson's ratio is not a reliable indicator of ductility. Moreover, relying solely on intrinsically-ductile elements to form HSD RHEAs is not sufficient, as such combinations can still experience brittle failure; it is also necessary to add the metric that HSD RHEAs use refractory elements with a wide range of radii. Finally, for a fast-prototyping optimization and validation approach, the application of advanced manufacturing, experiment, theory, and computational modeling [30] is recommended to tap the vast potential offered by RHEAs, as only a small fraction has been explored [1, 3].

ACKNOWLEDGMENTS

This paper describes objective technical results and analysis. Any subjective views or opinions that might be expressed in the paper do not necessarily represent the views of the U.S. Department of Energy or the United States Government. Sandia National Laboratories is a multimission laboratory managed and operated by National Technology & Engineering Solutions of Sandia, LLC, a wholly owned subsidiary of Honeywell International Inc., for the U.S. Department of Energy's National Nuclear Security Administration under contract DE-NA0003525.

The authors gratefully acknowledge the work done by all Organizing Committees of the International Conferences Nuclear Energy for New Europe.

REFERENCES

[1] O. Senkov et al., “Development and Exploration of Refractory High-entropy Alloys—A Review”, J. Mater. Res., Vol. 1, 2018.

[2] O. Senkov et al., “Ductile Nb alloys with reduced density and cost”, J. of Alloys and Compounds, Vol. 808, 2019.

[3] D. B. Miracle and O. N. Senkov, “A Critical Review of High-entropy Alloys and Related Concepts”, Acta Mater., Vol. 122, 2017, pp. 448-511.

[4] S. Dixit et al., “Refractory High-Entropy Alloy Thin Coatings for High Temperature Aerospace and Energy Applications,” J. of Thermal Spray Technology, Vol. 31, 2021, pp. 1021-1031.

[5] S. Rodriguez et al., “Application of Refractory High-Entropy Alloys for Higher-Reliability and Higher-Efficiency Brayton Cycles and Advanced Nuclear Reactors”, Sandia National Laboratories, SAND2021-11377, 2021.

[6] K. Kaufmann and K. S. Vecchio, 2020, “Searching for high entropy alloys: A machine learning approach”, Acta Materialia, Vol. 198, 2020, pp. 178-222.

[7] A. P. Mouritz, Introduction to Aerospace Materials, Woodhead Publishing Limited, Cambridge, 2012, pp. 463-464.

[8] N. Y. Stepanov et al., “Effect of Al on structure and mechanical properties of AlxNbTiVZr (x = 0, 0.5, 1, 1.5) high entropy alloys”, Materials Science and Technology, Institute of Materials, Minerals and Mining, Vol. 31, 2015A, pp. 1184-1193.

[9] C. Juan et al., “Solution strengthening of ductile refractory HfMoxNbTaTiZr high-entropy alloys”, Materials Letters, Vol. 175, 2016, pp. 284-287.

[10] L. Dirras et al., “Elastic and plastic properties of as-cast equimolar TiHfZrTaNb high-entropy alloy”, Mater. Sci. Eng. A, Vol. 654, No. 30, 2016.

[11] Y. D. Wu et al., “A refractory Hf25Nb25Ti25Zr25 high-entropy alloy with excellent structural stability and tensile properties”, Materials Letters, Vol. 130, 2014, pp. 277-280.

[12] X. Li et al., “Ductile and Brittle Crack-Tip Response in Equimolar High-Entropy Alloys”, Acta Materialia, Vol. 189, 2020, pp. 174-187.

[13] P. Cao et al., “Ab Initio Study of AlxMoNbTiV High Entropy Alloys”, J. of Physics Condensed Matter, Vol. 27, 2015, pp. 1-6.

[14] Y. D. Wu et al., “Phase composition and solid solution strengthening effect in TiZrNbMoV high-entropy alloys”, Materials & Design, Vol. 83, 2015, pp. 651-660.

[15] Z. An et al., “Spinodal Modulated Solid Solution Delivers a Strong and Ductile Refractory High-Entropy Alloy”, Materials Horizons, Vol. 8, 2021, pp. 948-955.

[16] S. Sheikh et al., “Alloy design for intrinsically ductile refractory high-entropy alloys”, J. Appl. Phys., Vol. 120, 2016, pp. 1-5.

[17] U. Bhandari, C. Zhang, and S. Yang, "Mechanical and Thermal Properties of Low-Density $Al_{20+x}Cr_{20-x}Mo_{20-y}Ti20V_{20+y}$ Alloys", Crystals, Vol. 278, 2020, pp. 1-9.

[18] B. S. Murty, J. W. Yeh, S. Ranganathan, and P. P. Bhattacharjee, High-Entropy Alloys, Elsevier, 2nd Ed., 2019, pp. 71, 73-75, and 93.

[19] T. Egami, W. Guo, P. D. Rack, and T. Nagase, "Irradiation Resistance of Multicomponent Alloys", The Minerals, Metals & Materials Society, Vol. 45A, 2014, pp. 180-183.

[20] A. Kustas and S. Rodriguez, Non-Provisional Patent, US62810723, "Refractory High Entropy Alloy Compact Heat Exchanger", 2019.

[21] S. Rodriguez, A. Kustas, and D. Ames, Provisional Patent, US62909901, "High-entropy Alloys, Refractory High-entropy Alloys, Methods of Selecting and Making, and Structures Formed from High-entropy and Refractory High-entropy Alloys", 2020.

[22] Z. An et al., "A Novel HfNbTaTiV High-Entropy Alloy of Superior Mechanical Properties Designed on the Principle of Maximum Lattice Distortion", J. of Materials Science & Technology, Vol. 79, 2021, pp. 109-117.

[23] W. Guo et al., "Microstructures and mechanical properties of ductile NbTaTiV refractory high entropy alloy prepared by powder metallurgy", J. of Alloys and Compounds, Vol. 776, 2019, pp. 428-436.

[24] W. D. Klopp, "Review of Ductilizing of Group VIA Elements by Rhenium and Other Solutes", NASA, TN D-4955, 1968.

[25] N. Y. Stepanov et al., "An AlNbTiVZr0.5 high-entropy alloy combining high specific strength and good ductility", Materials Letters, Vol. 161, 2015B, pp. 136-139.

[26] R. A. Romero, Investigation of Refractory High Entropy Alloys for Extreme Environment Applications, University of Texas at El Paso, Ph.D. Diss., Open Access Theses & Dissertations 3540, 2022.

[27] D. Ikeuchi et al., "A New Refractory and Transition Metal High-Entropy Alloy System", Scripta Materialia, Vol. 158, 2019, pp. 141-145.

[28] W. Guo et al., "Microstructures and mechanical properties of refractory MoNbHfZrTi high-entropy alloy", Materials & Design, Vol. 81, 2015, pp. 87-94.

[29] C. Lee et al., "Lattice distortion in a strong and ductile refractory high-entropy alloy", Acta Materialia, Vol. 160, 2018, pp. 158-172.

[30] S. Rodriguez, Applied Computational Fluid Dynamics and Turbulence Modeling: Practical Tools, Tips and Techniques, Springer International Publishing, 1st Ed., 2019, pp. 5-7.